


ORIGINAL ARTICLE

Open Access



Recirculation of Parallel-Connected Planetary Gear Trains

Hong Chen^{1*}  and Xiao-An Chen²

Abstract

Recirculation is expected to be identified for its possibility to dramatically decrease the efficiency of planetary gear trains (PGTs). However, it exhibits an unexplained connection with the structure, making it challenging to identify without tedious computation through tooth and speed ratios, thus complicating the design process. This study employs a generic model utilizing the mechanical balance principle and reveals the fundamental laws of the previously unexplained connection for parallel-connected ring-sun-type PGTs. Two necessary and sufficient conditions, torque and structure, were proven for multi-stage and two-stage PGTs without recirculation, respectively. This shows that the structure, specifically whether the links are central gears or carriers, and the connections between them directly impact the recirculation of these PGTs. A geometric model representing the structure and kinematics was developed to visualize the power flow. Thus, the recirculation of parallel-connected ring-sun-type PGTs can be predicted without calculations. Our results provide the underlying insights to understanding recirculation from the structural connection viewpoint, thereby contributing to the conceptual design phase where the task is to select the kinematic structure and the gear size is unknown.

Keywords: Power flow, Generic three-terminal, Torque direction, Multistage PGTs

1 Introduction

Most automatic transmissions for passenger cars use parallel-connected planetary gear trains. When designing such trains, the designer usually faces multiple candidate configurations during the conceptual design phase. Generally, these candidate configurations satisfy the motion design objectives. Therefore, efficiency often determines the final choice. However, an undesired pattern of power flow, recirculation, in these trains is believed to be one of the leading causes of lower efficiency compared with simple gear trains. Recirculation generates circulating power inside the PGTs. This portion of power does not produce a useful output. In some cases, it can produce several times more useless power consumption inside the trains than the input. Therefore, recirculation must be detected. At the very least, the allowed recirculation should not

exceed a specified limit. The unfavorable effects of recirculation in differential gear trains and continuously variable transmission were also reported by Pennestrì et al. [1].

Various methods have addressed power flow and recirculation in the context of efficiency, because a fundamental step in mechanical efficiency analysis is ascertaining the power flow direction [2] and verifying recirculation. Because the power flow within trains is a fundamental problem [3], there have also been studies devoted to the internal power flow of compound planetary gear trains [4–6]. The most direct power flow analysis method involves full static force and velocity analyses [7–9]. Another study used the sensitivity of the speed ratio to determine the direction of power flow [2, 10–13]. In this approach, the torque and angular speed were solved to determine the active and passive components. Some studies did not complete the static force analysis but used the gear ratio to calculate the power ratio [3, 14, 15]. Additionally, several concepts, including latent power

*Correspondence: hchen@mail.xhu.edu.cn

¹ School of Mechanical Engineering, Xihua University, Chengdu 610039, Sichuan, China

Full list of author information is available at the end of the article

[16, 17], virtual power [18, 19], and potential power, were used to determine the direction of the power flow on each meshing pair through the angular velocity calculated based on the gear ratio.

The feature of these studies is that the gear ratio/number of teeth is used as the essential parameter through which the subsequent kinematics and torque analysis can be carried out. Considering that the first factor is the choice of topology or structure [20] when a transmission is designed, it is reasonable to treat the topology or structure as a design variable. The limitation is that the structure is discrete and difficult to describe using a continuous function. Nevertheless, the topology or structure has an impact on the power flow. Kahraman et al. [7] believed that efficiency was closely related to the chosen kinematic configurations. Salgado mentioned the relationship between the power flow and structure of PGTs [11]. Gupta et al. [5] pointed out that power flow depends on planetary ratios, whereas the magnitude of planetary ratios is simultaneously a function of the type of planetary train and gear size. However, these studies did not provide details regarding the relationship or function of the structure/type of PGTs. Therefore, the question arises on the relationship between the power flow and structure.

The motivation of this study was to explore the unexhausted relationship between the discrete structure and power flow mentioned in previous studies. Research that has some relevance to the results is reported in Ref. [6] in which 16 assemblies (structures) of high-efficiency epicyclic gears were identified. However, the derivation in Ref. [6] was based on the parameters defined by the tooth number, and the results were limited to 1-DOF two-stage PGTs. For multistage PGTs, the combination of topologies leads to a significant increase in the number of assemblies (structures). Simultaneously, the nature of the combination causes the formula to be re-derived for each additional stage. Continuing to use the method described in Ref. [6], the calculation becomes very complicated and challenging. Therefore, a more conventional approach is to use a computer to simultaneously determine the speed and torque on all links of a given structure. However, in the conceptual phase, where one has to determine the basic structure from multiple candidates, the gear size has not been determined. Therefore, a method to identify the potential recirculation in multistage parallel-connected PGTs without knowing the gear size is desired. Such a method allows the prediction of performance in advance when only the structure is known. Thus, the results of the trial and error can be determined earlier, and the design process is accelerated. The work developed in this study contributes to the early phase of the design process.

This study considers only the ideal power flow because the friction loss is usually insufficient to change the power flow pattern [15]. By the power flow pattern, we mean the presence or absence of recirculation. The proposed approach is based on a geometrical model [21] to represent the structure and kinematics of the PGTs simultaneously. For this purpose, we extended the geometrical model to visualize the torque and power flow in this study.

The remainder of this paper is organized as follows. Section 2 presents a general model of multistage parallel-connected PGTs: Two interconnected generic three terminals. Section 3 presents the geometric model required for the power flow analysis. In Section 4, we prove the no-recirculation torque condition that should be satisfied by two interconnected generic three terminals. It is used as a fast examining tool for recirculation. We then applied this tool to the 2-stage case, resulting in a no-recirculation structure condition applicable to 2-stage parallel-connected PGTs. Section 5 explains the use of generic three-terminal and two necessary and sufficient conditions to analyze general PGTs through gear train decomposition in complex multistage gear train applications. Section 6 presents two examples including a complex 4-stage case.

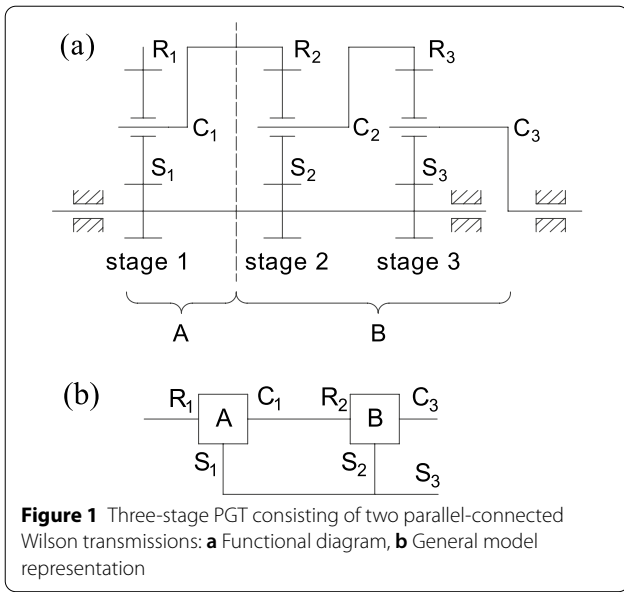
2 Parallel-connected Gear Train with Split Power

A PGT with multistage planetary gear sets is a typical compound gear train [18, 22]. White [6] reduced these trains to series-connected and parallel-connected PGTs, and pointed out that split power can be provided solely by parallel-connected PGTs.

The concept of parallel-connected PGTs was explained by Ross et al. [23]. In these trains, certain members are connected between the two adjacent stages. In the first and second stages shown in Figure 1(a), the sun gears, S_1 and S_2 , are connected together as one carrier and one ring gear, C_1 and R_2 .

Most parallel-connected PGTs used in automatic transmission use ring-sun-type planetary gear sets, although equivalent mechanisms can be obtained using external gear pair combinations. The disadvantages of using an external gear pair combination are that it cannot utilize the load capacity of the ring gear, requires a longer axial dimension, and has fewer types of interstage connections.

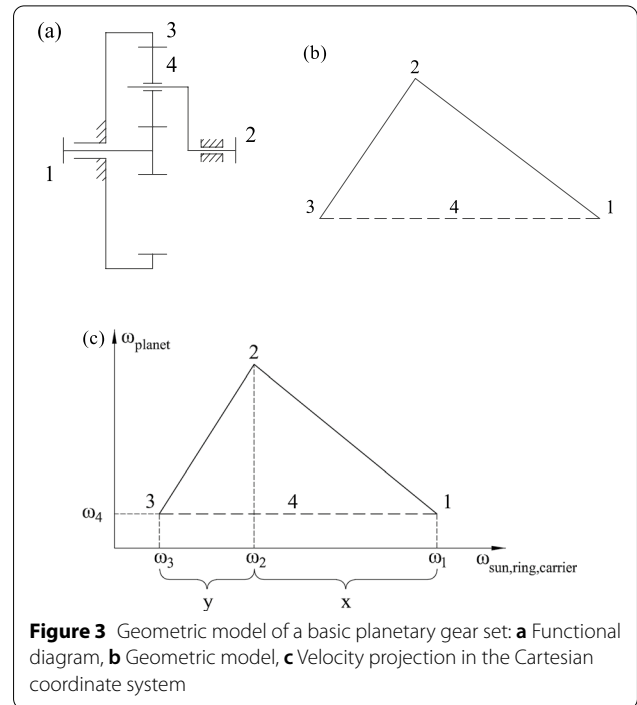
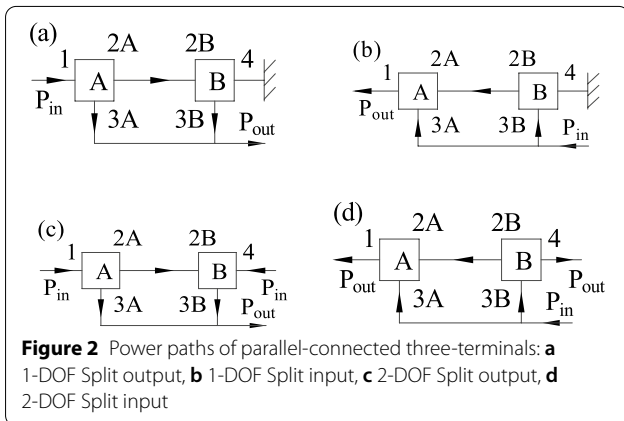
In the parallel-connected configuration, at most, there are two interconnections between any two adjacent stages, which would otherwise rotate as a single unit. Therefore, it is always possible to find the appropriate location to divide any multistage parallel-connected PGTs into two parts: each part is a generic three-terminal. Consequently, the split power of parallel-connected planetary gear trains can be represented by a generic



model consisting of two interconnected generic three terminals, as shown in Figure 1(b). Each generic three-terminal can be a basic planetary gear set or a 2-DOF planetary gear train in the general model.

Figure 2 illustrates the variations in the power split under this representation. Ports 2A and 2B constitute a power branch rotating freely, whereas ports 3A and 3B indicate a branch for output in Figure 2(a) and (c) and input in Figure 2(b) and (d), respectively. Notably, the generic models shown in Figure 2 are different from those in previous studies, where only two basic planetary gear sets were considered.

Figure 2(b) and (d) shows the inversions of Figure 2(a) and (c), respectively. Therefore, the analysis in this study is limited to Figure 2(a) and (c). The same result can be deduced from Figure 2(b) and (d).



3 Geometric Model of PGTs

3.1 Structure Representation

The power flow analysis of multistage PGTs usually requires the calculation of speed and torque. However, the number of teeth was not determined in the conceptual design stage. Therefore, a structural representation that can easily visualize the essential functions of the transmission without addressing the complexities of planetary gear kinematics is helpful. In this study, a geometric model was used as the analysis tool. It provides two functions: qualitative kinematics for power flow analysis and a structural representation for power flow visualization. Qualitative kinematics and structural representations are also physical meanings of the geometric model.

Figure 3 shows the functional diagram of a basic planetary gear set. Two fundamental circuits, 2-34 and 2-14, can be identified, according to Buchsbaum et al. [24].

The basic planetary gear set shown in Figure 3(a) can be represented as a geometric model in which the vertices represent the center link, including the sun, ring, and carrier, and the horizontal dashed line represents the planet, as shown in Figure 3(b). Each solid line in a geometric graph connects two vertices, one representing the central gear, and the other representing the carrier. This solid line is referred to as a circuit line because its vertices belong to the same fundamental circuit.

The fundamental circuit, represented by the circuit line, is the building block of the geometric model. According

to the definition of a fundamental circuit, planet 4 is shared by two fundamental circuits. Therefore, the horizontal dashed line 4 “connects” vertices 1 and 3 belonging to different fundamental circuits. Another link shared in Figure 3(a) is carrier 2, represented by the intersection point of the two circuit lines, as shown in Figure 3(b).

When a link is used as the central link in different fundamental circuits, we use a vertical dashed line to indicate its sharing. This type of sharing includes cases where it is used as a carrier and center gear or as different center gears in different fundamental circuits. An example of a more complex PGT represented by this sharing among the fundamental circuits is shown in Figure 4. In this train, link 2 is shared by fundamental circuits 2-35, 2-45, and 1-26. The intersection point of circuit lines 2-3 and 2-4 indicates that shared link 2 acts as a carrier in circuits 2-35 and 2-45. This intersection point is connected to the vertex of another circuit line 1-2 by a vertical dashed line. This vertical dashed line indicates that the function of link 2 in the other fundamental circuit, namely 1-26, is the central gear. Finally, because link 4 acts only as a common sun for fundamental circuits 2-45 and 1-46, two circuit lines, 1-4 and 2-4, are connected by a vertical dashed line on the vertices representing central gear 4.

As shown in Figures 3(b) and 4, the vertexes representing the ring gear are always on the circuit line with a positive slope, while the vertexes representing the sun gear are always on the circuit line with a negative slope. Therefore, there is a correspondence between the type of gear and slope of the circuit line. This is explained in Section 3.2 because of its kinematic meaning. In Figure 4, the dashed line between vertexes 1 and 2 is an auxiliary line [21] in which all the vertex representing carriers should be located.

3.2 Kinematics

In contrast to other representations, a geometric model was developed to directly represent the kinematics of PGTs based on their structural representation. Each

circuit line strictly corresponds to the Willis equation for the associated fundamental circuit. The slope of the circuit line is equal to the ratio of teeth in the Willis equation. The relationship between the positions of different circuit lines corresponds to the structural connections of the train. The lengths of the various circuit lines are determined by both the kinematic constraint of the train (isokinetic constraint) and structural connection. When equipped with Cartesian coordinates, the value of the horizontal projection of the dashed line representing the planet onto the vertical axis is the angular velocity of the planet, as shown by ω_4 in Figure 3(c). Similarly, the value of the vertical projection of the vertex representing the central link on the horizontal axis is the angular velocity of the central link, as shown by ω_3 , ω_2 , and ω_1 in Figure 3(b).

The representation of kinematics comes from the definite physical meaning of the slope of the circuit line: the tooth ratio of the center gear to the planet. Therefore, the circuit line represents the type of fundamental circuit, that is, the internal gear mesh or external gear mesh. Because the tooth ratios of the internal and external gear meshing pairs have different symbols, the slope of the circuit line is a signed number.

Let λ represent the slope of the circuit line, ω the angular velocity of the link, and Z the number of teeth in the gear. The kinematic equations [25] of a fundamental circuit can then be reformulated as

$$\begin{cases} \lambda_{sp} = \frac{\omega_p - \omega_c}{\omega_s - \omega_c} = -\frac{Z_s}{Z_p}, \\ \lambda_{rp} = \frac{\omega_p - \omega_c}{\omega_r - \omega_c} = +\frac{Z_r}{Z_p}, \end{cases} \quad (1)$$

where the subscripts s , r , p , and c denote the sun, ring gear, planet, and carrier, respectively. Because the dimensions of the ring gear are constant greater than those of the planet in the internal gear mesh, we obtain

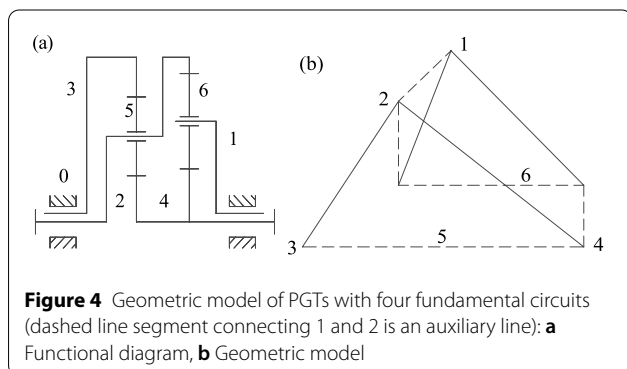
$$\lambda \begin{cases} = \lambda_{sp} < 0 & \text{external gear mesh,} \\ = \lambda_{rp} > 1 & \text{internal gear mesh.} \end{cases} \quad (2)$$

The tooth ratio of the ring gear to the sun within a planetary gear set can be expressed as follows through the geometric meaning of the slope of a straight line:

$$-\frac{Z_r}{Z_s} = \frac{x}{y} = \frac{\lambda_{rp}}{\lambda_{sp}}, \quad (3)$$

where x and y are the lengths of the vertical projection of the circuit line on the horizontal axis, as shown in Figure 3(c).

When only qualitative kinematics are desired, the slope of each circuit line is arbitrary under the constraint of the



structure, and Eq. (2). Nevertheless, it does not affect the correctness of the qualitative kinematics. Therefore, one can easily draw a geometric graph for a PGT. We used Figure 4 as an example to illustrate the steps of the geometric model drawing. Without loss of generality, the drawing begins with the first stage from the left.

Consider an arbitrary point in the plane as link 2. It is generally convenient to choose a carrier as the starting point for drawing. It is also permissible to begin with any other link.

Starting from link 2, draw a straight line to the lower left with an arbitrary slope greater than one. The length of the straight line was arbitrary and its endpoint was link 3. This step will provide fundamental circuit 2-35.

Starting from link 2, draw a straight line down to the right at any slope less than zero, until the endpoint has the same horizontal height as link 3. The end of the straight line is part of link 4, which belongs to the first planetary stage, that is, the sun of the first planetary stage. This step yields fundamental circuit 2-45.

Connecting 3 and 4 with a dashed line gives the planet 5.

Starting from 2, we draw a vertical dashed line of an arbitrary length. The endpoint of the vertical dashed line is still link 2. However, it indicates the part of link 2 that belongs to the second planetary stage, that is, the ring of the second planetary stage.

Starting from the ring of the second planetary stage, draw a straight line to the upper right with an arbitrary slope greater than 1 and intersect the (imaginary) auxiliary line with slope 1. The intersection point is the other carrier (link 1). It should be noted that if an imaginary auxiliary line is drawn, it should be drawn as a dashed line. This step gives fundamental circuit 1-26.

Starting from 1, draw a straight line to the lower right, with the endpoint being the intersection of the horizontal dashed line passing ring 2 and the vertical dashed line passing sun 4. This is the sun of the second planetary stage. The straight line gives fundamental circuit 1-46. The horizontal dashed line between the newly obtained point and ring 2 corresponds to planet 6. It should be noted that the slope of straight line 1-4 is not arbitrary. This is naturally constrained by the previous steps.

The qualitative kinematics of the train are determined from the geometric model: the angular velocity of all central links increases from left to right, and the angular velocity of all planets increases from bottom to top. When any central link is fixed, the rotation of the other central links is reversed on both sides.

This study does not deal with the exact kinematic solution. When the exact solution needs to be obtained, the geometric model must be placed in a Cartesian coordinate system, and the slope of each circuit line must be given.

From the above process of drawing the geometric model, it is clear that the geometric graph is unique when the slopes of all the circuit lines are given. For a detailed explanation of the geometric method and exact solution of the kinematics, refer to Ref. [21].

3.3 Torque Analysis

Eliminating the planet speed from Eq. (1) returns the Willis' ratio. Together with the power balance and torque balance equation [15] of the fundamental circuit, Willis' ratio leads to a well-known result for a fundamental circuit: the torque ratios of the three shafts are functions of Willis' ratio. Several studies have documented these results.

In this study, we considered only PGTs of the ring-sun type because of the parallel-connected constraint. For the basic planetary gear set shown in Figure 3, the above result leads to a definite relationship of the signs among the torques of the fundamental links: the torques of the sun and ring have the same sign, and they are opposed to that of the carrier. This relationship can be expressed in the context of the geometric method using Eq. (3):

$$\frac{T_s}{T_r} = \frac{y}{x}, \tag{4}$$

$$T_c = -\left(\frac{x+y}{x}\right)T_r, \tag{5}$$

and

$$T_c = -\left(\frac{x+y}{y}\right)T_s. \tag{6}$$

Considering the torque balance on the planet, Eq. (4) can be graphically expressed as shown in Figure 5.

4 Conditions of Torque and Structure without Recirculation

By definition, power is the product of the speed and torque. The sign of this product determines the direction of the power flow. Therefore, to analyze the direction of the power flow and determine the presence of recirculation, we do not need specific values for the velocity, torque, and power. The geometric model provides the relative magnitude and direction of the velocities. Eqs. (4), (5), and (6) formulate the relationship between the torque directions of the three basic links in the planetary gear set. Therefore,

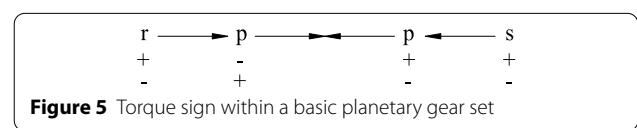


Figure 5 Torque sign within a basic planetary gear set

combined with the mechanical balance principle, it is possible to analyze the power flow and recirculation directly using a geometric model based on the definition of power. However, for multistage parallel-connected PGTs, direct analysis is still cumbersome and does not provide more insight into the conditions for the presence or absence of recirculation. This section uses the general model proposed in Section 2 to treat parallel-connected PGTs of arbitrary stages, consisting of two interconnected generic three terminals, and proves the no-recirculation condition for the general model. The results of this section provide a new theoretical approach for the fast determination of recirculation. It is worth noting that the proof uses only the definition of power and the principle of mechanical equilibrium, and does not involve the number of stages, kinematics, and structural connections within the generic three-terminal. Therefore, the generic three-terminal in this section was used as a black box, and the internal kinematics and structure were arbitrary.

4.1 Condition of Torque without Recirculation for Coupled Generic Three-terminals

1-DOF. In this study, the input torques were assumed to have the same sign as the angular velocities. Therefore, the power flowing in the system was considered to have a positive sign.

Figure 2(a) shows the power flow pattern without recirculation. Ports 2A and 2B, 3A and 3B were isokinetic, respectively. Hence, with the given power flow shown in Figure 2(a), the torque direction is opposite for ports 2A and 2B, and the same for ports 3A and 3B.

We then consider the inverse proposition of the consequence deduced above.

Table 1 lists the variations in the directions of the angular velocity and torque within power branch 2A-2B. Because there is no additional power source or load for ports 2A and 2B, it can be observed from Table 1 that cases III and IV are not physically reasonable. Cases I and II are physically practical because the

opposite power is present in ports 2A and 2B to produce a flow of power.

The direction variations of the angular velocities and torques within branch 3A-3B are listed in Table 2. Similar to Table 1, it can be observed that Cases II, III, V, VII, and VIII are not physically reasonable. Among the remaining three cases, Case I was the only configuration of torque directions to produce power flow without recirculation, whereas Cases IV and VI were not.

After excluding the physically unreasonable cases, we can then combine the no recirculation cases in Tables 1 and 2. The only possible configuration for no recirculation was Case I in Tables 1 and 2, which is the inverse proposition of the consequence deduced above. Thus, the necessary and sufficient condition that the torques should be satisfied in a 1-DOF two-stage parallel-connected generic three-terminal without recirculation can be concluded as follows:

C1: Under physically allowed circumstances, the same torque direction holds for two ports belonging to a split input or output branch.

Isokinetic ports 2A and 2B always maintain opposite directions of torque and the same torque amplitudes, regardless of the pattern of power flow. This is known as the balance condition and is useful in the analysis of power flow without calculation.

Nevertheless, it should be noted that the balance condition is a special case for the configuration shown in Figure 2(a). Consider a more general case of introducing a fictitious power source or load onto the 2A-2B branch. Obviously, in cases III and IV in Table 2, recirculation still cannot be formed owing to the lack of an internal closed path. However, in cases I and II in Table 2, a closed power path can be developed to generate power flow if the torque direction between 2A and 2B is the opposite. In this case, the torque amplitudes of 2A and 2B may not be equal. Therefore, the basis for condition C1 is the opposite torque direction between 2A and 2B, which

Table 1 Variation for directions of torque and power within power branch 2A-2B

Case	Power of ports	Angular velocity	Torque	Power on branch	Practical
I	P _{2A} <0, P _{2B} >0	$\omega > 0$	T _{2A} <0, T _{2B} >0	Flow	Y
		$\omega < 0$	T _{2A} >0, T _{2B} <0		
II	P _{2A} >0, P _{2B} <0	$\omega > 0$	T _{2A} >0, T _{2B} <0	Flow	Y
		$\omega < 0$	T _{2A} <0, T _{2B} >0		
III	P _{2A} >0, P _{2B} >0	$\omega > 0$	T _{2A} >0, T _{2B} >0	No source	N
		$\omega < 0$	T _{2A} <0, T _{2B} <0		
IV	P _{2A} <0, P _{2B} <0	$\omega > 0$	T _{2A} <0, T _{2B} <0	No sink	N
		$\omega < 0$	T _{2A} >0, T _{2B} >0		

Table 2 Variation for directions of torque and power within power branch 3A-3B

Case	Power flow in link 2	Power flow in link 3	Angular velocity	Torque	Power on branch/gear set
I	P2A<0, P2B>0	P3A<0, P3B<0	$\omega > 0$ $\omega < 0$	T3A<0, T3B<0 T3A>0, T3B>0	Flow to output
II		P3A<0, P3B>0	$\omega > 0$ $\omega < 0$	T3A<0, T3B>0 T3A>0, T3B<0	Inconsumable for set B
III		P3A>0, P3B>0	$\omega > 0$ $\omega < 0$	T3A>0, T3B>0 T3A<0, T3B<0	Inconsumable for set B and no output on link 3
IV		P3A>0, P3B<0	$\omega > 0$ $\omega < 0$	T3A>0, T3B<0 T3A<0, T3B>0	Recirculation
V	P2A>0, P2B<0	P3A<0, P3B<0	$\omega > 0$ $\omega < 0$	T3A<0, T3B<0 T3A>0, T3B>0	No source for set B
VI		P3A<0, P3B>0	$\omega > 0$ $\omega < 0$	T3A<0, T3B>0 T3A>0, T3B<0	Recirculation
VII		P3A>0, P3B>0	$\omega > 0$ $\omega < 0$	T3A>0, T3B>0 T3A<0, T3B<0	Inconsumable for set A and no output on link 3
VIII		P3A>0, P3B<0	$\omega > 0$ $\omega < 0$	T3A>0, T3B<0 T3A<0, T3B>0	Inconsumable for set A and no source for set B

produces a power flow. For convenience, we refer to this as the equilibrium condition.

However, the amplitude of the torques of ports 3A and 3B may be unequal because they connect to an outer output. The overall output torque and one of the output ports are denoted by T_{out} and α , respectively, and the other output port is $T_{out} - \alpha$. Thus, a compact power flow classification based on the output torque can be expressed as follows:

$$\begin{cases} 0 < \alpha < T_{out} \wedge 0 < (T_{out} - \alpha) < T_{out} & \text{no recirculation,} \\ \alpha < 0 \wedge (T_{out} - \alpha) > T_{out} & \text{recirculation,} \\ \alpha > T_{out} \wedge (T_{out} - \alpha) < 0 & \text{recirculation.} \end{cases} \quad (7)$$

Suppose T_{out} is positive (by positive, we mean that the direction makes the power of the output link output power). When the inversion of Figure 2(b) is considered, the same conclusion can be deduced by replacing T_{out} with T_{in} :

$$\begin{cases} 0 < \alpha < T_{in} \wedge 0 < (T_{in} - \alpha) < T_{in} & \text{no recirculation,} \\ \alpha < 0 \wedge (T_{in} - \alpha) > T_{in} & \text{recirculation,} \\ \alpha > T_{in} \wedge (T_{in} - \alpha) < 0 & \text{recirculation.} \end{cases} \quad (8)$$

2-DOF. Condition C1 is also valid for the 2-DOF split output/input, as shown in Figure 2(c) and (d), and the proof process is similar. The difference is that case V in Table 2 is symmetrical with case I; therefore, case V is valid and without recirculation.

It should be noted that the proof of C1 is exhaustive in its approach, although it has two forms. The reason for using the exhaustive method instead of the analytic

method is that the nature of the topology is discrete and there is no uniform formula. Therefore, the general model established in Section 2 has an advantage: it allows the exhaustion of all possible variations at a small cost.

Additionally, this section does not involve a geometric model, and the torque condition without recirculation exists independently of the geometric model.

4.2 Conditions of Structure without Recirculation for 2-stage PGTs

Consider two coupled generic three terminals; each one should provide two ports for interconnection. Hence, it is deduced immediately from C1 and the balance condition that one three-terminal should produce the same torque directions for its two ports. In contrast, the other provides opposite torque directions, so that there is no recirculation. As shown in Figure 6, the balance condition forces the torque on the free-rotating branch to reverse the sign once, and the internal reverse sign of the second three-terminal eventually leads to the same torque sign for the two input/output ports. It should be noted

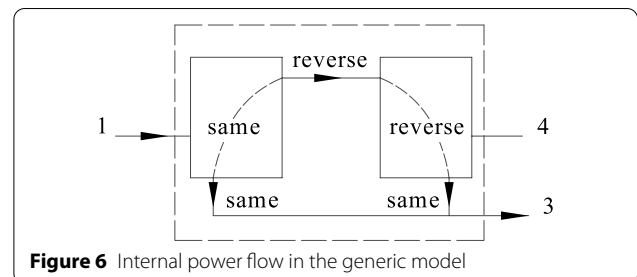


Figure 6 Internal power flow in the generic model

that the degree of freedom of port 4 has been released in Figure 6, and the input or fixed status of port 4 does not affect the above inverse sign process. According to the generic three-terminal definition, the torque relationship of the ports in Figure 6 is valid regardless of the number of basic planetary sets they contain.

Using the deduction above, the structural condition that was obeyed by the two connections between the two basic planetary gear sets to form a 2-stage parallel-connected PGT of the ring-sun type without recirculation can be drawn by inserting the relationships described in Eqs. (4), (5) and (6) in Figure 6.

C2: One connection joins a carrier and a central gear, whereas the other joins two central gears.

It is noteworthy that the derivation of C1 and C2 uses the relative velocity of the links, which are dependent on the sign of Willis' ratio and the connection between the links but does not use the information on the change in the number of teeth and speed ratio. This means that the existence of recirculation for parallel-connected PGTs of the ring-sun type could be identified by internal connections without performing calculations.

5 Multistage Parallel-connected PGTs

The multistage parallel connection is mainly used in automatic transmissions, where the gear train, control elements, and casing form a mechanism with three, four, or more degrees of freedom. However, with respect to the gear train, the given action of the control elements will cause the gear train itself to form a single degree-of-freedom planetary gear train in each gear. Therefore, it is reasonable to apply conditions C1 and C2 to the multistage parallel-connected PGTs. Local two-stage recirculation is identified by C2, where the link type is checked. The recirculation across multiple stages is identified by C1, where the structural connections are analyzed to determine the torque direction of the ports of the generic three terminals.

Consider any gear. If the degree of freedom connected to the casing is released, the corresponding gear train becomes a 2-DOF parallel-connected PGT. In this case, the total number of connections between basic planetary sets is $2n-2$, where n is the number of basic planetary gear sets. Therefore, there are at least one and at most two interconnections between two adjacent basic planetary gear sets.

For such a PGT, one can always find a suitable position and divide the gear train into two halves to apply C1: each part should be a generic three-terminal. By checking the structural connection relationship, the torque direction of the four ports can be derived from the input or output step-by-step to determine whether recirculation occurs across multiple stages.

Furthermore, for each generic three-terminal, the segmentation continues until the smallest unit can be applied with C2, and the possible local recirculation can then be identified.

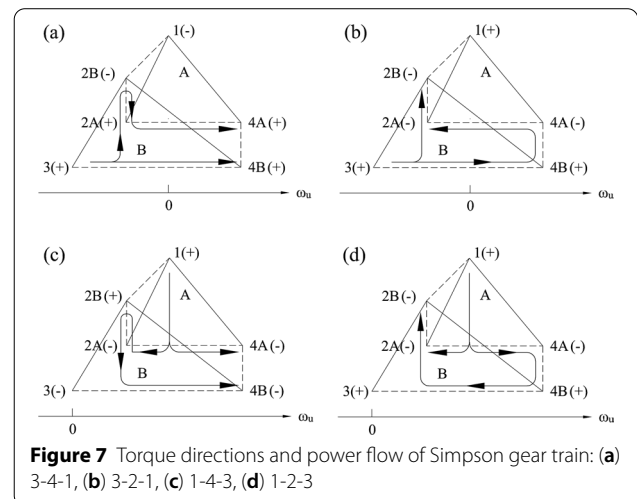
Finally, by combining the kinematics that are visualized by the geometric model and the torque direction derived above, the directions of recirculation and power flow can be determined precisely without knowing the gear size. Section 6 illustrates this application with examples.

6 Examples

Two structures, one without recirculation and another with recirculation, were selected for the analysis. The first example aims to verify C2 and illustrate the power flow analysis using a geometric model where only the structural connections are known. The power flow is analyzed without calculation through the relative velocity and torque sign relationship, whereas the torque amplitudes are calculated using Eqs. (4), (5), and (6) to verify C2. First, the power flow was analyzed for an arbitrary split-output configuration. Then, the torque amplitudes were calculated for the contrary configuration to fully evaluate the split output and its inversion. The second example illustrates the application of C1 and C2 to complicated multistage parallel-connected PGTs.

6.1 Simpson Gear Train

According to C2, the Simpson gear train shown in Figure 4 is without recirculation. The geometric graphics in Figure 4(b) are redrawn in Figure 7 to visualize the torque directions under different input and output configurations. The notation $j-k-m$ is used to represent the different configurations, where j represents the input link, k represents the output link, and m represents the ground link. The horizontal axis in Figure 7 represents the relative velocities



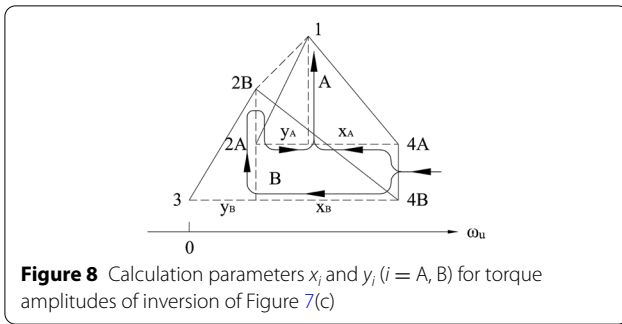


Figure 8 Calculation parameters x_i and y_i ($i = A, B$) for torque amplitudes of inversion of Figure 7(c)

of the central gear and carrier. The positive sign in parentheses indicates the torque direction, which is the same as the input torque, and the negative sign indicates the torque direction, which is contrary to the input torque.

One of the keys to analyzing power flow without calculation is that the kinematics of PGTs, including the angular velocity direction and relative magnitude, are directly available by the geometric model. For example, the angular velocity of link 1 in Figure 7(a) is zero, because link 1 is the ground link. Therefore, the angular velocity of link 4 is greater than zero, and those of links 2 and 3 are less than zero. Similarly, one can deduce that the absolute value of the angular velocity of link 3 was higher than that of link 2.

Figure 7(c) shows the configuration of 1-4-3. A positive torque is needed to make the power on link 1 the input because the input angular velocity is greater than zero. According to Eqs. (5) and (6), the torques at ports 2A and 4A are negative. To produce a flow of power and balance the power within branch 2A-2B, the torque of port 2B should be positive, and that of port 4B should be negative. Consequently, ports 4A and 4B had the same torque direction. The angular velocity directions of input link 1 and output link 4 are the same because they lie on the same side as the ground link 3. Therefore, the power of link 4 is negative, which satisfies the definition of the output power.

According to the directions of the angular velocity and torque, it is easy to determine the direction of power flow according to the definition, as indicated by the heavy line with arrows. The arrows in Figure 7 indicate that there is no recirculation in the parallel power paths under any of the four input/output configurations.

Figure 8 shows the inversion of the configuration shown in Figure 7(c). Let T_4 and T_{4A} be T_{in} and α , respectively. Then T_{4B} will be $T_{in} - \alpha$. According to Eqs. (4) and (6), we obtain:

$$T_{2A} = \frac{x_A}{y_A} T_{4A} = \frac{x_A}{y_A} \alpha, \tag{9}$$

and

$$T_{2B} = -\frac{x_B + y_B}{y_B} T_{4B} = -\frac{x_B + y_B}{y_B} (T_{in} - \alpha). \tag{10}$$

By the balance conditions and identical deformations, we can obtain

$$\alpha = \frac{(x_B + y_B)/y_B}{(x_A/y_A + (x_B + y_B)/y_B)} T_{in}. \tag{11}$$

Because x_i and y_i ($i = A, B$) only represent the length, the torque of input port T_{4A} satisfies $0 < \alpha < T_{in}$; hence, the torque of port T_{4B} satisfies $0 < (T_{in} - \alpha) < T_{in}$. This result is consistent with that obtained using Eq. (8), and Figure 8 is a configuration without recirculation.

As an extension of this example, one can find that all 16 assemblies in Ref. [6] satisfy the condition C2.

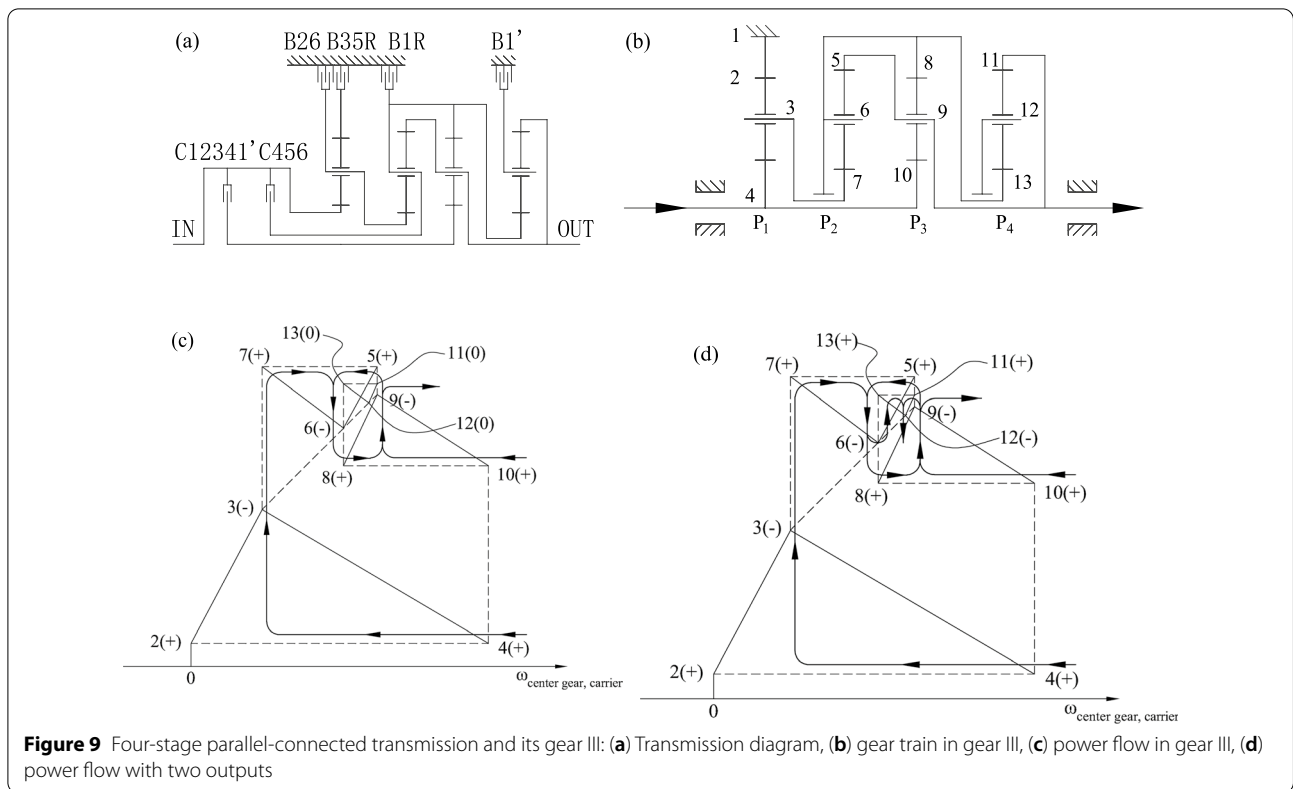
6.2 Four-stage Parallel-connected Automatic Transmission

Figure 9 shows the 3-DOF automatic transmission developed by Xie et al. [26] for heavy-duty commercial and military vehicles. The gear train corresponding to gear III is illustrated in Figure 9(b).

Only one direct interconnection exists between the basic planetary gear sets P1 and P2. It is possible to divide P1 and P2 and view gear sets P2, P3 and P4 as a generic three-terminal of 2-input 1-output. Within this generic three-terminal, the basic planetary gear sets P2 and P3 do not satisfy condition C2. Because link 12 does not consume power, planetary gear set P4 is bypassed, and there is a recirculation between P2 and P3.

We then examined the recirculation between the two generic three terminals. For the generic three-terminal, where the input is located, the torque on carrier 3 is negative because the torque on input 4 is positive, as shown in Eq. (6). For the generic three-terminal consisting of P2, P3, and P4, the torque on sun 7 is negative based on the balance principle. Because the torque on output 9 is negative, the torque on sun 10 is positive according to Eq. (6). At this point, the torques on the ports of the two generic three terminals are known. From the torque direction on these four ports, it is known from C1 that there is no recirculation between the two generic three terminals, that is, between P1 and P2.

Consider the following more complicated situation: a load is applied to link 12. In this case, because link 13 is connected to links 6 and 8, the structural condition cannot be utilized directly. However, the power flow is between links 6 and 8 as long as the torque directions are opposite. Thus, C2 can be utilized directly. It should be noted that the torque direction on link 7 is the same as that on link 10 because it reverses twice from the input.



Therefore, the torque signs of links 6 and 8 must be opposite, and recirculation must occur between P2 and P3.

The power flows in both cases are shown in Figure 9(c) and (d) and are obtained by the same method as in the above example. In both cases, there was indeed a recirculation path 9-5-6-8-9 between P2 and P3.

7 Conclusions

This study analyzes the recirculation of parallel-connected PGTs of the ring-sun type from the perspective of the structure, that is, the internal interconnection within the PGTs. The difference between our idea and previous research is that the entire multistage PGT is treated as a generic model composed of two interconnected generic three terminals. The possible closed power path is abstracted by the generic model, thereby avoiding the discussion of the diversity of topology structures and complex kinematics of multistage PGTs, which are the main limitations faced by the previous methods using the gear ratio. The torque condition without recirculation that should be satisfied by the internal interconnections of generic three terminals is then proved by energy balance and is applied to the simplest parallel-connected two-stage PGTs to deduce the corresponding structural condition. The two conditions provide different insights from the past and a specific link between the structure

and recirculation for this type of PGT. Thereby, possible recirculation can be identified based on an analysis of the structure. Although the torque sign relationship within the basic planetary gear set is well known, its use with a new model for the structure and kinematic representation of PGTs shows that the flow direction of power can be visualized without knowing the tooth number. Two examples verify the conditions of the torque and structure and show the application of complicated multistage PGTs.

The approach proposed in this work can be applied to the fast evaluation of gear transmission designs and contribute to the most difficult conceptual design stage.

Acknowledgements

Not applicable.

Authors' contributions

HC wrote the manuscript; XC provided advice on the manuscript. All authors have read and approved the final manuscript.

Authors' Information

Hong Chen, born in 1971, is currently an associate professor at *Xihua University, China*. He received his Ph.D. from *Chongqing University, China*, in 2012. His research interests include electromechanical transmission and precision measurement.

Xiao-An Chen, born in 1956, is currently a professor at *the State Key Laboratory of Mechanical Transmission, Chongqing University, China*. He received his Ph.D. from *Chongqing University, China* in 1999. His research interests include high-performance transmissions and intelligent equipment.

Funding

Supported by the Spring Light Program of the Ministry of Education of the People's Republic of China (Grant No. Z2016129), and Educational Commission of Sichuan Province of China (Grant No. 15202441).

Competing interests

The authors declare no competing financial interests.

Author Details

¹School of Mechanical Engineering, Xihua University, Chengdu 610039, Sichuan, China. ²The State Key Laboratory of Mechanical Transmissions, Chongqing University, Chongqing 400044, China.

Received: 12 August 2020 Revised: 20 January 2022 Accepted: 22 March 2022

Published online: 05 April 2022

References

- [1] E Pennestrì, L Mariti, P P Valentini, et al. Efficiency evaluation of gearboxes for parallel hybrid vehicles: Theory and applications. *Mechanism and Machine Theory*, 2012, 49: 157–176.
- [2] J M del Castillo. The analytical expression of the efficiency of planetary gear trains. *Mechanism and Machine Theory*, 2002, 37(2): 197–214.
- [3] E Pennestrì, F Freudenstein. A systematic approach to power-flow and static-force analysis in epicyclic spur-gear trains. *Journal of Mechanical Design*, 1993, 115(3): 639–644.
- [4] C Chen. Power flow analysis of compound epicyclic gear transmission: simpson gear train. *Journal of Mechanical Design*. 2011, 133(9): 945021–945025.
- [5] A K Gupta, C P Ramanarayanan. Analysis of circulating power within hybrid electric vehicle transmissions. *Mechanism and Machine Theory*, 2013, 64: 131–143.
- [6] G White. Derivation of high efficiency two-stage epicyclic gears. *Mechanism and Machine Theory*, 2003, 38(2): 149–159.
- [7] A Kahraman, H Ligata, K Kienzle, et al. A Kinematics and power flow analysis methodology for automatic transmission planetary gear trains. *Journal of Mechanical Design*, 2004, 126(11): 1071–1081.
- [8] F Yang, J Feng, H Zhang. Power flow and efficiency analysis of multi-flow planetary gear trains. *Mechanism and Machine Theory*, 2015, 92: 86–99.
- [9] E L Esmail, S S Hassan. An approach to power-flow and static force analysis in multi-input multi-output epicyclic-type transmission trains. *Journal of Mechanical Design*, 2010, 132(1): 0110091–01100910.
- [10] R A Lloyd. Power flow and ratio sensitivity in differential systems. *Proceedings of the Institution of Mechanical Engineers, Part D: Journal of Automobile Engineering*, 1991, 205(1): 59–67.
- [11] D R Salgado, J M del Castillo. Selection and design of planetary gear trains based on power flow maps. *Journal of Mechanical Design*, 2005, 127(1): 120–134.
- [12] T Ciobotaru, D Frunzeti, I Rus, et al. Method for analysing multi-path power flow transmissions. *Proceedings of the Institution of Mechanical Engineers, Part B: Journal of Engineering Manufacture*, 2010, 224(9): 1447–1454.
- [13] D R Salgado, J M del Castillo. Analysis of the transmission ratio and efficiency ranges of the four-, five-, and six-link planetary gear trains. *Mechanism and Machine Theory*, 2014, 73: 218–243.
- [14] G Del Pio, E Pennestrì, P P Valentini. Kinematic and power-flow analysis of bevel gears planetary gear trains with gyroscopic complexity. *Mechanism and Machine Theory*, 2013, 70: 523–537.
- [15] E Pennestrì, F Freudenstein. The mechanical efficiency of epicycle gear trains. *Journal of Mechanical Design*, 1993, 115(3): 645–651.
- [16] D Yu, N Beachley. On the mechanical efficiency of differential gearing. *Journal of Mechanisms Transmissions and Automation in Design*, 1985, 107(1): 61–67.
- [17] L C Hsieh, H C. Tang. On the meshing efficiency of 2K-2H type planetary gear reducer. *Advances in Mechanical Engineering*, 2015, 5(5): 686187.
- [18] C Chen. Power flow and efficiency analysis of epicyclic gear transmission with split power. *Mechanism and Machine Theory*, 2013, 59: 96–106.
- [19] C Chen, T T Liang. Theoretic study of efficiency of two-DOFs of epicyclic gear transmission via virtual power. *Journal of Mechanical Design*, 2011, 133(3): 0310071–0310077.
- [20] Z Lévai. Structure and analysis of planetary gear trains. *Journal of Mechanisms*, 1968, 3: 131–148.
- [21] X A Chen, H Chen. Analytical geometry method of planetary gear trains. *Science China Technological Sciences*, 2012, 55(4): 1007–1021.
- [22] R Mathis, Y Remond. Kinematic and dynamic simulation of epicyclic gear trains. *Mechanism and Machine Theory*, 2009, 44(2): 412–424.
- [23] C S Ross, W D Route. A method for selecting parallel-connected, planetary gear train arrangements for automotive automatic transmissions. *SAE Technical Paper Series*, 1991, 911941.
- [24] F Buchsbaum, F Freudenstein. Synthesis of kinematic structure of geared kinematic chains and other mechanisms. *Journal of Mechanisms*, 1970, 5(3): 357–392.
- [25] R J Willis. On the kinematics of the closed epicyclic differential Gears. *Journal of Mechanical Design*, 1982, 104(4): 712–719.
- [26] T L Xie, J B Hu, Z X Peng, et al. Synthesis of seven-speed planetary gear trains for heavy-duty commercial vehicle. *Mechanism and Machine Theory*, 2015, 90(8): 230–239.

Submit your manuscript to a SpringerOpen[®] journal and benefit from:

- Convenient online submission
- Rigorous peer review
- Open access: articles freely available online
- High visibility within the field
- Retaining the copyright to your article

Submit your next manuscript at ► [springeropen.com](https://www.springeropen.com)